An Experimental Assessment of Direct Torque Control and Model Predictive Control Methods for Induction Machine Drive

Abdelkarim Ammar, Aissa Kheldoun, Brahim Metidji, Billel Talbi, Tarek Ameid, Younes Azzoug

An Experimental Assessment of Direct Torque Control and Model Predictive Control Methods for Induction Machine Drive

Abdelkarim AMMAR[1], Aissa KHELDOUN[1], Brahim METIDJI[1], Billel TALBI[2], Tarek AMIED[3], Younes AZZOUG[3]
[1]Signals and Systems Laboratory LSS, Institute of Electrical and Electronic Engineering, University M'hamed Bougara of Boumerdes, Boumerdes, Algeria.
[2]Laboratory of Power Electronics and Industrial Control, University of Sétif 1, Sétif, Algeria.
[3]Electrical Engineering Laboratory of Biskra LGEB, University of Biskra, Biskra, Algeria.
ammar.abdelkarim@yahoo.fr, aissa.kheldoun@univ-boumerdes.dz, metidji77@yahoo.fr, bilel_ei@live.fr, tarek-gnr@hotmail.fr, azzougyounes@yahoo.fr

***Abstract*– Finite-State Model Predictive Control methods (FS-MPC) have been presented recently in the field of electrical drive and power electronics as an alternative to the conventional strategies. This paper presents a comparative evaluation between Direct Torque Control (DTC) and two finite-state model predictive control strategies applied to induction motor drive. Both DTC and MPC are nonlinear control techniques which dispense with the use of modulation unit (i.e. pulse width modulator (PWM) or space vector modulator (SVM)). DTC can provide good decoupled flux and torque control using pair of hysteresis comparators and look-up switching table for voltage vectors selection. In contrast with the model predictive control which includes the inverter model in control design. The optimal selection of inverter switching states minimizes the error between references and the predicted values of control variables by the optimization of a cost function. The effectiveness of applied algorithms is investigated by an experimental implementation using real-time interface (RTI) based on dSpace 1104.**

Keywords— Induction Motor (IM), Direct Torque Control (DTC), Predictive Current Control (PCC), Predictive Torque Control (PTC), dSpace 1104.

I. INTRODUCTION

The Direct Torque Control (DTC) replaces the field oriented control (FOC) in the variable frequency drives field [1], [2]. DTC came up with simpler scheme, faster response and less dependence to machine parameters. However, due to the reliance on hysteresis comparators for flux and torque control and a switching table for voltage vectors selection. This strategy suffers from high torque and flux ripples and current harmonics. These ripples result in power quality deterioration and acoustical noises. Consequently, lower performance of the controlled machine especially at low speed operations.

In order to enhance the DTC performances and overcome the aforementioned drawbacks, numerous suggestions have been presented in literature in the last few decades. The application of artificial intelligence techniques and the use of multilevel converters were among the most conspicuous mentioned alternatives [3], [4]. Besides, the space vector modulation (SVM) was a very promising solution. The space vector modulation based direct torque control (SVM-DTC) preserves a constant switching frequency that reduces torque/flux ripples and hence switching losses [5]. However, this algorithm uses the stator field orientation control (SFOC) and linear PI controllers. In fact, SFOC requires the use of coordinate transformations which increases control algorithm complexity, while linear controllers are very sensitive to system parameters variation that deteriorate control robustness.

Recently, another method has been appeared and attracted a wide attention in the area of power converters and drives which is known by the Model Predictive Control (MPC)[6], [7]. Nowadays, MPC has become very popular research topic. It can be classified into two main categories, named by the continuous model predictive control and finite-state model predictive control (FS-MPC) [8]. The continuous MPC like the classical generalized predictive control (GPC) can demonstrate good performance. However, it has high order of complexity and needs a modulator in control design [9]. Contrariwise, the finite-state MPC, known as finite-control-set in other reference, (FCS-MPC), eliminates the use of modulation block, it incorporates the converter model in the control design and respects its discrete nature [6]. The converter switching states are considered in order to minimize a predefined cost function which consists of the errors between references and predicted measured control variables. The main disadvantage of MPC is the huge online computation effort, Fortunately, the use of digital signal processing (DSP) and the development of Field Programmable Gate Arrays (FPGAs) have made it possible to use MPC in fast dynamic process industries such as power electronics and control of electrical drives

The well applied finite-state model predictive control strategies for IM drive, are the predictive current control (PCC) and the predictive torque control (PTC) [6], [7]. PCC is expressed in the rotor field-oriented reference where the coordinates transformation is a necessary process, whilst, PTC is featured by stationary reference frame and keeps similar structure of traditional DTC, where the switching table is replaced by the online optimization procedure [10]. In finite state MPC, the control variables such as stator current in case of PCC or torque and flux in case of PTC are predicted for the finite number of possible switching states of a power converter [11]. The optimal selection of switching states which is obtained by actuating the cost function can reduce torque and flux ripples being the main DTC drawback. Then, the selected state is directly applied to the converter in the next sampling time [12].

In this paper, a comparative evaluation between direct torque and two-mentioned model predictive control methods is

presented. The experimental validation has been carried out using Matlab/Simulink software with dSpace 1104 real-time interface for the purpose of investigating control algorithms performance.

II. Induction Machine and Voltage Inverter Modelling

A. IM Model

The dynamic model of the induction machine can be expressed in the stationary frame in complex form by the following equations, where (1), (2) and (3) present voltage, flux and electromagnetic equations respectively:

$$\begin{cases} \bar{v}_s = R_s \bar{i}_s + \dfrac{d\bar{\psi}_s}{dt} \\ 0 = R_r \bar{i}_r + \dfrac{d\bar{\psi}_r}{dt} - j\,\omega_r \bar{\psi}_r \end{cases} \quad (1)$$

$$\begin{cases} \bar{\psi}_s = L_s \bar{i}_s + M_{sr} \bar{i}_r \\ \bar{\psi}_r = M_{sr} \bar{i}_s + L_r \bar{i}_r \end{cases} \quad (2)$$

$$T_e = p \cdot \mathrm{Im}\left\{\bar{\psi}_s \cdot \bar{i}_s\right\} \quad (3)$$

Where:

$\bar{v}_s$ is the stator voltage vector.

$\bar{\psi}_s$ and $\bar{\psi}_r$ are the stator flux and rotor flux vectors.

$\bar{i}_s$ and $\bar{i}_r$ are the stator and rotor currents vectors.

R_s and R_r are the stator and rotor resistances.

L_s, L_r and M_{sr} are stator, rotor and mutual inductance.

ω_r is the electrical velocity.

p is the number of pole pairs.

B. Two-Level Voltage Source Inverter Model

Two-level voltage source inverter (VSI) is considered in the present work to feed the induction motor. The generated output voltage of VSI can be expressed by:

$$V_s = \sqrt{\frac{2}{3}} V_{dc} \left[S_a + S_b e^{j\frac{2\pi}{3}} + S_c e^{j\frac{4\pi}{3}} \right] \quad (4)$$

V_{dc}: is the DC link voltage

The inverter's control bases on the logic values S_i.
with: i= *a, b, c.*

There are eight possible positions from the combinations of switching states. Six are active vectors (*V1, V2 ... V6*) and two are zero vectors (*V0, V7*). These eight switching states are shown as space vectors in Fig.1.

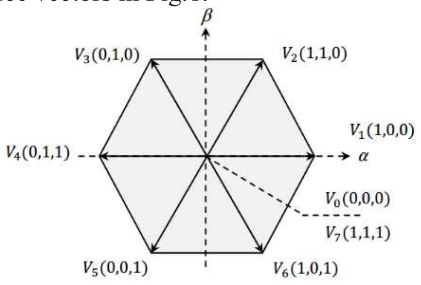

Fig.1 Two-level VSI voltage vectors in the complex plane.

III. Switching Table-Direct Torque Control (ST-DTC)

The direct torque control depends on switching table for the selection of an appropriate voltage vector. This selection is related directly to the variation of the stator flux and the torque. The relationship between the stator voltage and the stator flux change can be established as:

$$\Delta\psi_s = V_s T_z \quad (5)$$

From (5), we can deduce that the stator flux can be varied by the application of stator voltage during time T_z. During one sampling period, the rotor flux vector is supposed invariant. Then, the torque of induction motor can be expressed in terms of stator and rotor flux vectors as follows:

$$|T_e| = p \frac{M_{sr}}{\sigma L_s L_r} |\psi_s| |\psi_r| \sin(\delta) \quad (6)$$

where:

δ load angle between the stator and rotor flux vectors

According to (6), the torque can be controlled by adjusting the load angle δ if the stator and rotor flux amplitudes are maintained constant. Two and three level hysteresis comparators are used for flux and torque control.

The control scheme of conventional direct torque control using switching table is shown in Fig.2

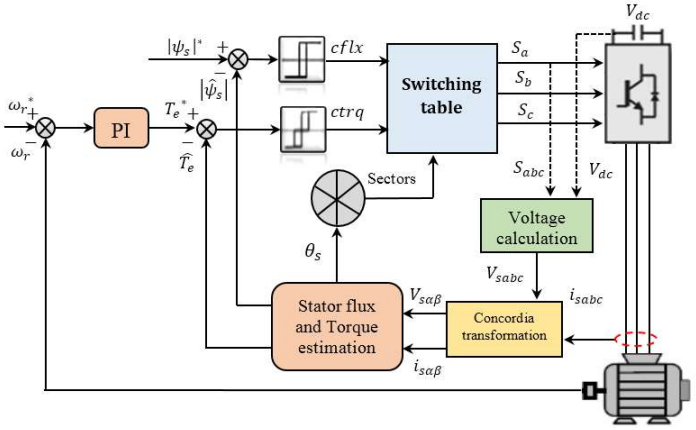

Fig.2 Global diagram of the switching table-based direct torque control.

IV. Model Predictive Control Moethds

In this section, two main MPC methods are presented, i.e. predictive current control (PCC) and predictive torque control (PTC). Both methods have the merits of MPC; however, they have different control variables in cost functions

A. Finite-state predictive current control (FS-PCC)

The predictive current control uses the field orientation as the basic vector control. From the IM model, the stator current expression can be given as follows:

$$\bar{i}_s = -\frac{1}{R_\sigma}\left(L_\sigma \cdot \frac{d\bar{i}_s}{dt} - k_r \cdot \left(\frac{1}{T_r} - j\,\omega \right) \bar{\psi}_r \right) - \bar{v}_s \quad (7)$$

Where:

$k_r = M_{sr}/L_r$, $R_\sigma = R_s + k_r^2 \cdot R_r$, $L_\sigma = \sigma . L_s$

The stator currents are predicted with all feasible voltage vectors, and these predictions are evaluated through a cost function [13].

To predict the next-sampling time *(k+1)* of the required signals, the Euler forward discretization is used:

$$\frac{dx}{dt} \approx \frac{x(k+1)-x(k)}{T_z} \tag{8}$$

After discretization with the sampling time T_z, the stator current prediction can be obtained as:

$$\bar{i}_s(k+h)=\left(1-\frac{T_z}{T_\sigma}\right)\cdot\bar{i}_s(k)+\frac{T_z}{T_\sigma}\cdot \frac{1}{R_\sigma}\left(k_r\cdot\left(\frac{1}{T_r}-j\,\omega(k)\right)\bar{\psi}_r(k)+\bar{v}_s(k)\right) \tag{9}$$

with:

$T_\sigma = \sigma L_s / R_\sigma$

h *is* the predictive horizon. In this section one step is considered (*h=1*).

The generation of the current references is necessary for PCC design. The expressions of direct and quadratic current components which are responsible for flux and torque producing can be given in rotor flux reference as follow:

$$i_{sd}^{*}=\frac{\left|\psi_r^{*}\right|}{M_{sr}} \tag{10}$$

$$i_{sq}^{*}=\frac{L_r T_e^{*}}{M_{sr}\left|\psi_r^{*}\right|} \tag{11}$$

The cost function design for PCC requires the current values in $\alpha\beta$ frame, therefore, the inverse Park transformation should be applied.

The cost function in the MPC strategy compares the predicted and reference quantities [8]. Then, the classical cost function of PCC is presented as follows:

$$g=\left|i_{s\alpha}^{*}-i_{s\alpha}(k+h)\right|+\left|i_{s\beta}^{*}-i_{s\beta}(k+h)\right| \tag{12}$$

Since a two-level inverter is used in this system, the cost function only needs to be calculated 7 times because the inverter has 7 different voltage vectors (Fig.1). The global block diagram of the PCC method is presented in Fig.3.

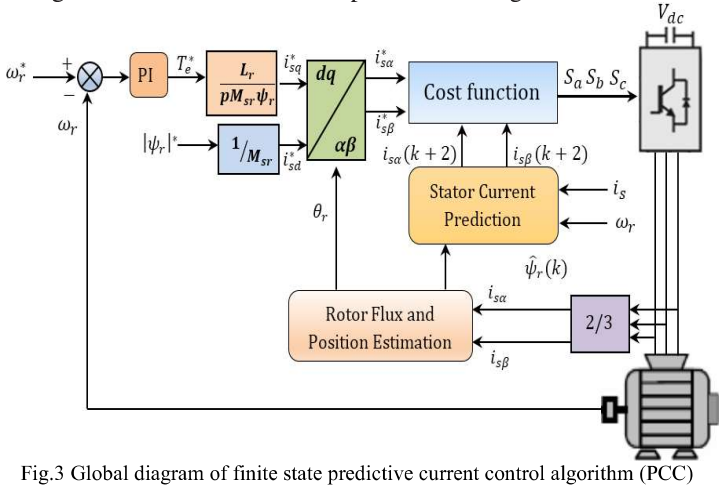

Fig.3 Global diagram of finite state predictive current control algorithm (PCC)

B. *Finite-state predictive torque control (FS-PTC)*

FS-PTC algorithm includes three main steps. The estimation of flux and torque. Then, the prediction of the next-instant of current $\bar{i}_s(k+1)$, flux $\hat{\bar{\psi}}_s(k+1)$ and torque $\hat{T}_e(k+1)$.Finally, The cost function design is done [11].

By using the same prediction method as the PCC algorithm, the predicted stator current and flux can be obtained as:

$$\bar{i}_s(k+h)=\left(1-\frac{T_z}{T_\sigma}\right)\cdot\bar{i}_s(k)+\frac{T_z}{T_\sigma}\cdot \frac{1}{R_\sigma}\left(k_r\cdot\left(\frac{1}{T_r}-j\,\omega(k)\right)\bar{\psi}_r(k)+\bar{v}_s(k)\right) \tag{13}$$

$$\hat{\bar{\psi}}_s(k+h)=\hat{\bar{\psi}}_s(k)+T_z\bar{v}_s(k)-R_s\cdot T_z\bar{i}_s(k) \tag{14}$$

The predicted electromagnetic torque can be calculated using the predicted current and flux as following:

$$\hat{T}_e(k+h)=p\cdot\mathrm{Im}\left\{\hat{\bar{\psi}}_s(k+h)\cdot\bar{i}_s(k+h)\right\} \tag{15}$$

The classical cost function for the PTC method is:

$$g=\left|T_e^{*}-\hat{T}_e(k+h)\right|+\lambda\left|\bar{\psi}_s^{*}-\hat{\bar{\psi}}_s(k+h)\right| \tag{16}$$

λ is the weighting factor, traditionally is defined as the trade-off between the torque and flux magnitudes[12].

Fig.4 shows the global diagram of PTC method.

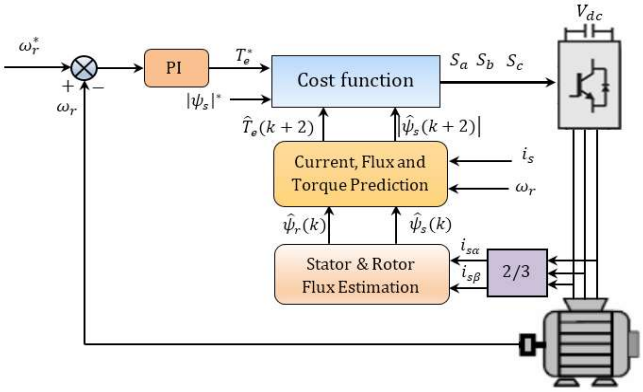

Fig.4 Global diagram of finite state predictive torque control algorithm (PTC)

C. *Cost function extension in FS-MPC algorithms*

FS-MPC is featured by a very flexible cost function, hence, it can be extended by adding other control objectives and system constraints. For example, current limitation term I_m is added to the cost function in order to protect over current through the stator. This term is designed according to the maximum supportable current by the machine [12], [14] as follows:

$$I_m=\begin{cases}\infty, & if\ \left|\bar{i}_s(k+h)\right|>i_{\max}\\ 0, & if\ \left|\bar{i}_s(k+h)\right|\le i_{\max}\end{cases} \tag{17}$$

i_{max} is the maximum current rating of the IM. Thus, the complete cost functions g for the PCC and PTC controllers are:

$$g=\left|i_{s\alpha}^{*}-i_{s\alpha}(k+h)\right|+\left|i_{s\beta}^{*}-i_{s\beta}(k+h)\right|+I_m \tag{18}$$

$$g=\left|T_e^{*}-\hat{T}_e(k+h)\right|+\lambda\left|\bar{\psi}_s^{*}-\hat{\bar{\psi}}_s(k+h)\right|+I_m \tag{19}$$

D. Time-delay compensation in model predictive control

In simulation, the different measurements are taken at the discrete instant *k*, and at the same time the optimum voltage vector $\vec{v}_s(k)$ is applied to the machine. However, in a real implementation the processor needs time to execute the algorithm. It takes one sampling cycle to generate the optimum switching state if the variables are measured at time *k*. Accordingly, the optimum actuating variables are given to the inverter at the time step *k+1*, and not at step *k* as in simulation. Therefore, a delay time compensation should be conducted.

The predictive horizon *h* will be considered by two-step ahead with (*h=2*) instead one step. Consequently, the instant *(k+1)* will be considered as an initial condition for the predictions at instant (*k+2*).

By considering the calculation delay in real time implementation, the cost functions of PCC and PTC respectively become now:

$$g = \left|i_{s\alpha}^{*} - i_{s\alpha}(k+2)\right| + \left|i_{s\beta}^{*} - i_{s\beta}(k+2)\right| + I_m \quad (20)$$

$$g = \left|T_e^{*} - \hat{T}_e(k+2)\right| + \lambda\left|\vec{\psi}_s^{*} - \hat{\vec{\psi}}_s(k+2)\right| + I_m \quad (21)$$

V. Experimental Implemntation

The real-time implementation was done in the laboratory equipped by dSpace 1104 interface. The experimental test rig of IM drive is composed, as shown in (Fig.5), of: 1: A squirrel-cage IM *1.1 kW*. 2: power electronics Semikron converter composed of a rectifier and an IGBT based voltage source inverter. 3: speed sensor (type: incremental encoder). 4: dSpace dS 1104 with 5: Matlab/Simulink/Controldesk software plugged in personal computer. 6: magnetic powder brake with load control unit. 7: Hall type current sensors.8: DC-bus voltage sensors. 9: numerical oscilloscope.

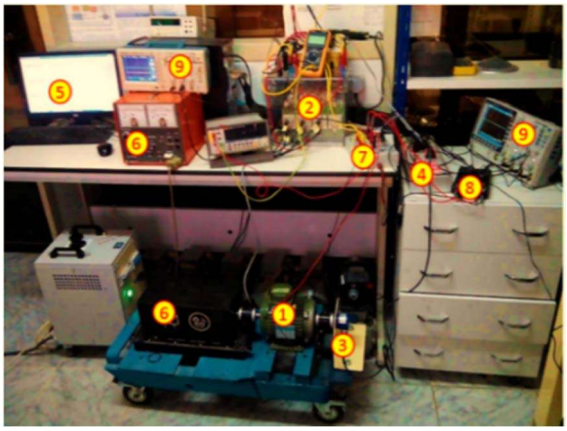

Fig.5 Presentation of the experimental setup.

The results have been extracted using GW-INSTEK numerical oscilloscope which is linked to dSpace RTI. The adopted same sampling frequencies is 10 kHz. The performance analysis is done as comparative evaluation between the conventional switching table DTC strategy (ST-DTC) and two finite state model predictive control methods (i.e. PCC and PTC), where: "a" for DTC, "b" for PCC, "c" for PTC.

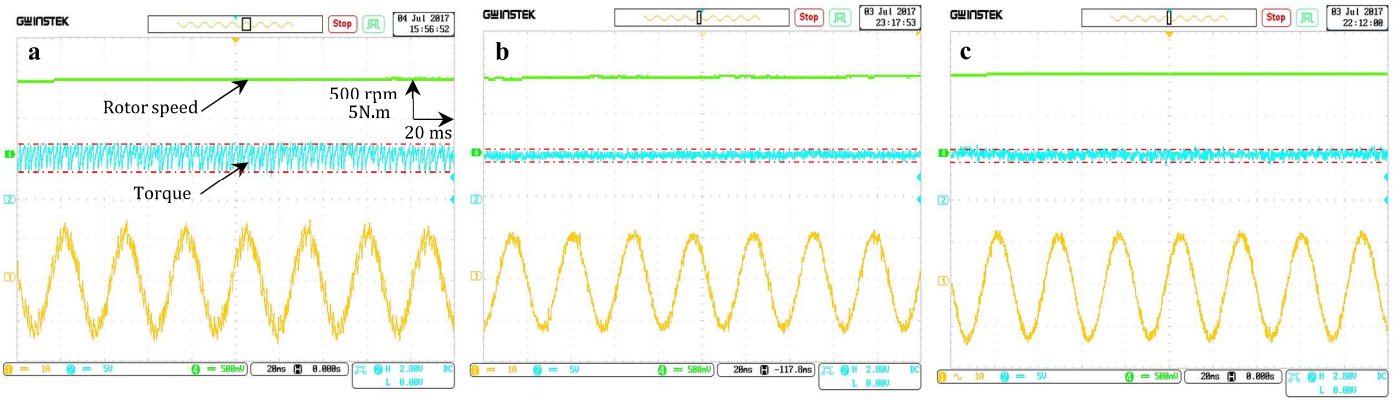

Fig.6 Steady state under load condition: Rotor speed [rpm], Torque [N.m], Stator phase current [A].

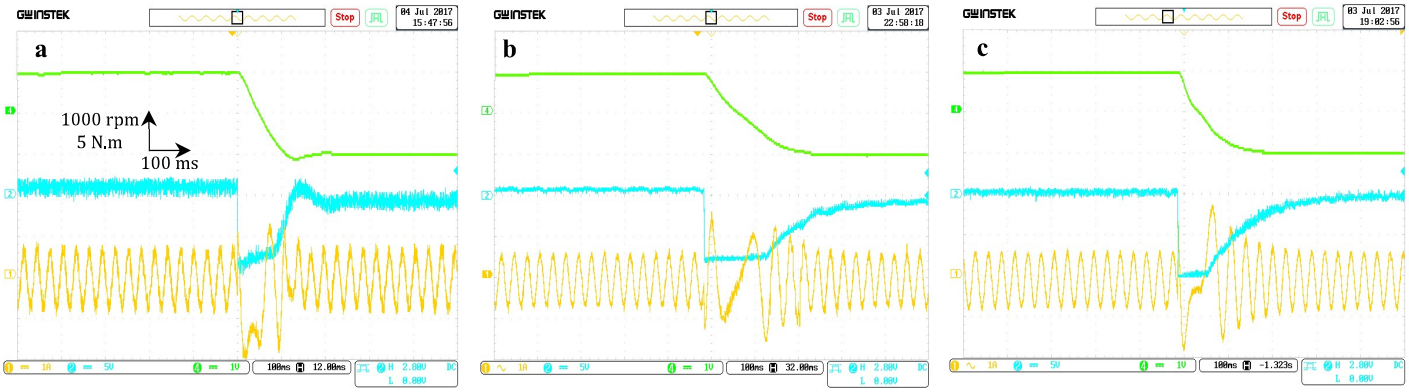

Fig.7 Rotation reversing maneuver: Rotor speed [rpm], Torque [N.m], Stator phase current [A].

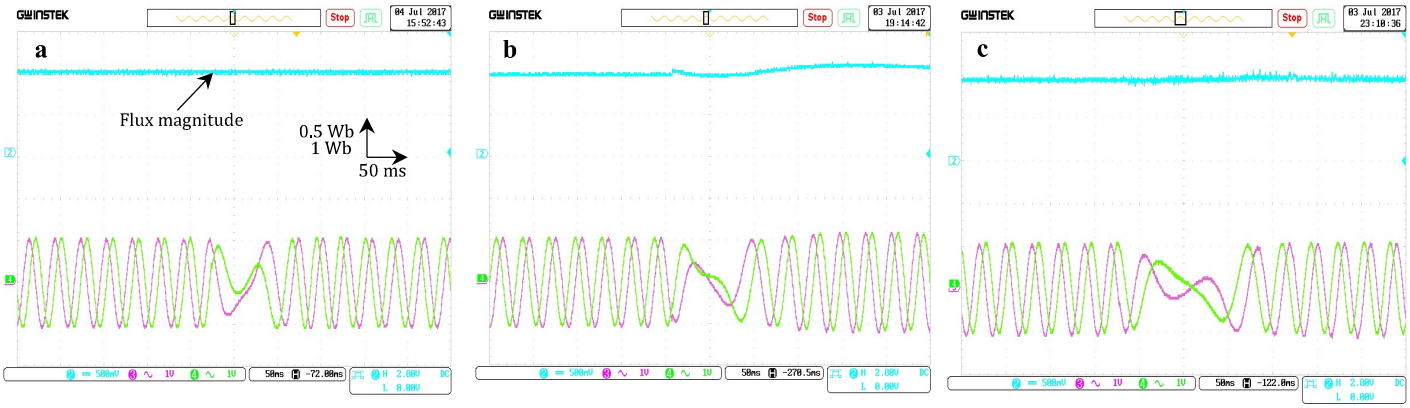

Fig.8 Rotation reversing maneuver: Flux magnitude and flux componants [Wb].

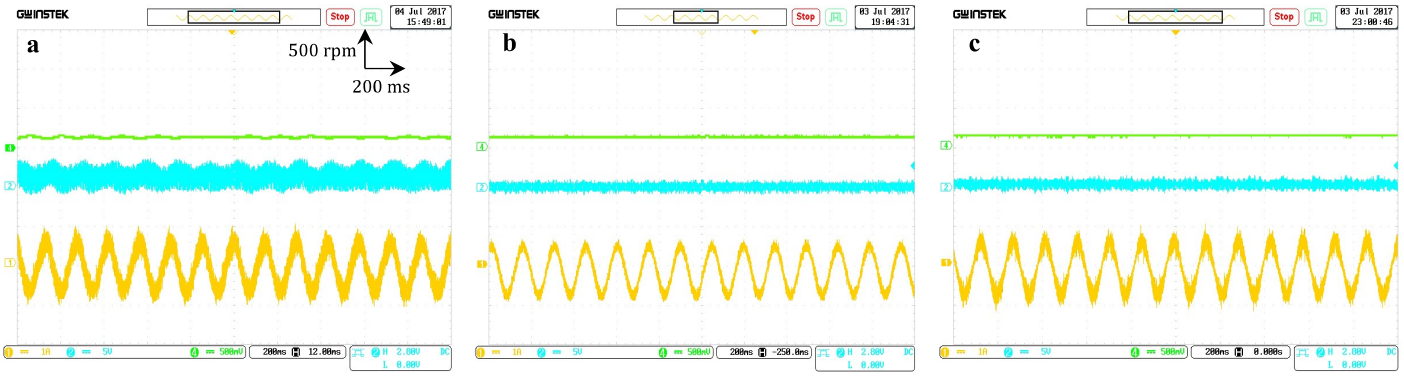

Fig.9 Low speed operation: Rotor speed [rpm], Torque [N.m], Stator phase current [A].

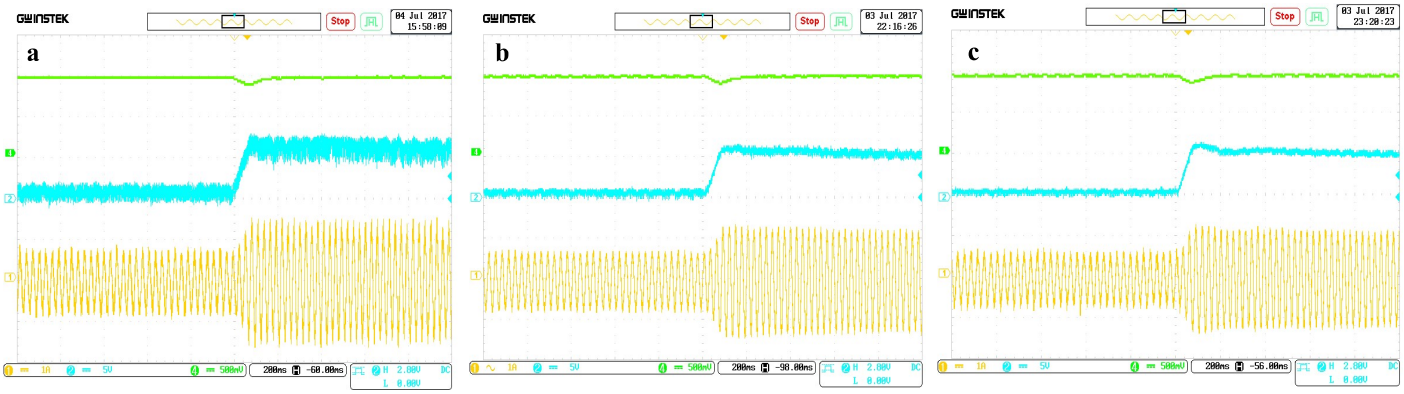

Fig.10 Load application condition : Rotor speed [rpm], Torque [N.m], Stator phase current [A].

The displayed figures above show different devlopped operation tests, which are, the steady state behavior, speed reversal maneuver, low speed operation and torque response to load application. Figs.6 (a-b-c) presnets the steady state of the three control stratgies at speed of 1000 rpm and load of 5N.m. The figures depict from top to bottom, rotor speed, torque and stator phase current. DTC shows good speed tracking but high torque ripples (± 2 N.m) and current harmonics. However, PCC and PTC have much better current quality and reducer torque ripples (±0.35 N.m). Then Fig.7 compares the perfromance while the rotation sense is reversing. The control stratgies have a simular behavoir, where the system is opeared at the physical limit during the reversing. DTC and PTC show fast dynamic. PCC shows a good current wavefrom and low torque ripples. Fig.8 presents the flux evolution under the reversal maneuver. Figs.8 (a-c) show the stator flux magnitude and components for DTC and PTC while Fig.8 (b) shows the rotor flux for PCC. PCC and PTC show smoother flux magnitude, however, the rotor flux magnitud of PCC has been affected by the speed reversing.

Next, in Figs.9 (a-b-c) the low speed region has been conducted. The machine operates with rotor speed of 200 rpm and without load. The figures show from top to bottom, rotor speed, torque and stator current. In Fig.10(a), we can observe that the torque of DTC strategies has been extremely deformed, the rotor speed shows some fluctuations and current harmonics have been increased. Generally, in DTC strategy at low speeds, the machine becomes unstable, the torque performance is diminished and speed regulation maybe inaccurate. In the other hand, the model predictive control techniques show good

behavior at low speed region, especially PCC which has the best current quality. The last operation condition which has been conducted is the load application. Fig.10 presents rotor speed, torque and current with load introduction of 5 N.m. Since the same anti-windup PI controller has been adopted for the external speed loop in all control strategies, they have a similar speed/torque response and load rejection. It can be seen that DTC has high ripples while PTC than PCC show a reducer torque ripples due to the optimal selection of voltage vector by the cost function optimization.

In general, the theoritcal and the experimental analysis show that PCC and PTC have minimized flux and torque ripples in spite of the fact that they operate with switching frequency as DTC. PCC control design needs coordinate transformation unlike DTC and PTC. However, this technique has the lowest calculation burden and the simplest scheme which does not require flux and torque estimation. In addition, no parameters must be adjusted. Moreover, PCC has the best current quality, while PTC, has the reduced torque ripples but needs weighting factors design.

In spite of some mentioned disadvantages of model predictive control techniques, the high flexibility of the cost function design makes it easy to handle system constraints for the sake of performance enhancement. Then, Table.1 below concludes the comparison of the all presented control algorithms.

Table.1 Comparative analysis of DTC, PCC and PTC.

	DTC	PCC	PTC
Switching frequency	Variable	Variable	Variable
Calculation	Low	Low	Average
Modulation	No	No	No
Torque ripples	High	Low	Lowest
Current quality	Bad	Better	Good
Coordinate transformation	No	Required	No
Angle estimation	Required	Required	No

VI. CONCLUSION

In this paper, a comparative evaluation of conventional direct torque control and finite-state predictive control methods is carried out for two-level voltage source inverter fed induction machine. The presented control methods have been verified through real-time implementation using dSpace 1104 board. Different operation tests have been conducted in order to investigate the performances such as steady state, speed direction reversing, low speed operation and load application.

According to both theoretical and experimental aspects, all presented control techniques are featured by the absence of inner PI loops and the modulation unit. However, the most remarkable property of MPC methods is that they offer reduced ripples and better current waveform; despite the fact that they operate under a variable switching frequency as DTC.

Generally, the finite state model predictive control techniques are presented as the new alternative solution in electrical drives and power electronics field. They preserve numerous good proprieties of conventional drives and offer more advantages. Nevertheless, they still a challenging subject for researches concerning performance enhancement.

APPENDIX

The parameters of the three-phase Induction motor, employed for simulation and real implementation, in SI units are:

1.1kW, *50 Hz*, $p=2$, $R_s=6.75\Omega$, $R_r=6.21\Omega$, $L_s=L_r=0.5192$ H, $M_{sr}=0.4957$ H, $f_r=0.002$ SI, $J=0.01240$ kg.m^2.

REFERENCES

[1] I. Takahashi and T. Noguchi, "A New Quick-Response and High-Efficiency Control Strategy of an Induction Motor," *Ind. Appl. IEEE Trans.*, vol. IA-22, no. 5, pp. 820–827, 1986.

[2] D. Casadei, F. Profumo, G. Serra, and A. Tani, "FOC and DTC: Two viable schemes for induction motors torque control," *IEEE Trans. Power Electron.*, vol. 17, no. 5, pp. 779–787, 2002.

[3] V. N. N, A. Panda, and S. P. Singh, "A Three-Level Fuzzy-2 DTC of Induction Motor Drive Using SVPWM," *IEEE Trans. Ind. Electron.*, vol. 63, no. 3, pp. 1467–1479, Mar. 2016.

[4] Yongchang Zhang, Jianguo Zhu, Zhengming Zhao, Wei Xu, and D. G. Dorrell, "An Improved Direct Torque Control for Three-Level Inverter-Fed Induction Motor Sensorless Drive," *IEEE Trans. Power Electron.*, vol. 27, no. 3, pp. 1502–1513, Mar. 2012.

[5] A. Ammar, A. Bourek, and A. Benakcha, "Sensorless SVM-Direct Torque Control for Induction Motor Drive Using Sliding Mode Observers," *J. Control. Autom. Electr. Syst.*, vol. 28, no. 2, pp. 189–202, Apr. 2017.

[6] J. Rodriguez, J. Pontt, C. A. Silva, P. Correa, P. Lezana, P. Cortes, and U. Ammann, "Predictive Current Control of a Voltage Source Inverter," *IEEE Trans. Ind. Electron.*, vol. 54, no. 1, pp. 495–503, Feb. 2007.

[7] P. Correa, M. Pacas, and J. Rodriguez, "Predictive Torque Control for Inverter-Fed Induction Machines," *IEEE Trans. Ind. Electron.*, vol. 54, no. 2, pp. 1073–1079, Apr. 2007.

[8] S. Vazquez, J. Rodriguez, M. Rivera, L. G. Franquelo, and M. Norambuena, "Model Predictive Control for Power Converters and Drives: Advances and Trends," *IEEE Trans. Ind. Electron.*, vol. 64, no. 2, pp. 935–947, Feb. 2017.

[9] P. Alkorta, O. Barambones, J. A. Cortajarena, and A. Zubizarrreta, "Efficient Multivariable Generalized Predictive Control for Sensorless Induction Motor Drives," *IEEE Trans. Ind. Electron.*, vol. 61, no. 9, pp. 5126–5134, Sep. 2014.

[10] Y. Zhang, B. Xia, and H. Yang, "Model predictive torque control of induction motor drives with reduced torque ripple," *IET Electr. Power Appl.*, vol. 9, no. 9, pp. 595–604, Nov. 2015.

[11] A. Ammar, B. Talbi, T. Ameid, Y. Azzoug, A. Kerrache, A. Bourek, and A. Benakcha, "Predictive direct torque control with reduced ripples and fuzzy logic speed controller for induction motor drive," in *2017 5th International Conference on Electrical Engineering - Boumerdes (ICEE-B)*, 2017, pp. 1–6.

[12] M. Habibullah and D. D.-C. Lu, "A Speed-Sensorless FS-PTC of Induction Motors Using Extended Kalman Filters," *IEEE Trans. Ind. Electron.*, vol. 62, no. 11, pp. 6765–6778, Nov. 2015.

[13] F. Wang, X. Mei, P. Tao, R. Kenne, and J. Rodriguez, "Predictive Field-Oriented Control for Electric Drives," *Chinese J. Electr. Eng.*, vol. 3, no. 1, pp. 73–78, 2017.

[14] F. Wang, S. Li, X. Mei, W. Xie, J. Rodriguez, and R. M. Kennel, "Model-based predictive direct control strategies for electrical drives: An experimental evaluation of PTC and PCC methods," *IEEE Trans. Ind. Informatics*, vol. 11, no. 3, pp. 671–681, 2015.